Hidden electronic state of CuO revealed by resonant inelastic x-ray scattering

Hisashi Hayashi* and Yasuo Udagawa
IMRAM, Tohoku University, Katahira, Sendai 980-8577, Japan

W. A. Caliebe and C.-C. Kao
NSLS, Brookhaven National Laboratory, Upton, New York 11973
(Received 20 March 2002; published 3 July 2002)

High-resolution resonant inelastic x-ray scattering (RIXS) spectra from CuO in the $1s2p$ emission region were measured. A surprisingly complicated set of spectra was observed. Detailed analysis of these spectra reveals the existence of an excited state, which is hidden in the Cu-*K* x-ray absorption spectrum of CuO. Furthermore, the energy of this excited state corresponds well to a Cu $4p_z$-like state predicted by a real-space multiple-scattering technique, but has not been observed experimentally up to now. This result demonstrates the potential use of RIXS to complement x-ray absorption spectroscopy.

DOI: 10.1103/PhysRevB.66.033105 PACS number(s): 78.70.Ck, 78.70.Dm, 74.72.−h

Understanding the electronic structures of strongly correlated transition metal oxides has been one of the long-standing challenges in condensed matter physics. The study of these oxides has attracted renewed interest recently due to the discovery of high-*Tc* superconductors. Among them, divalent CuO is of particular importance because it shares the same basic building block, CuO_4 parallelogram plane, with high-*Tc* materials, which makes CuO a good model system towards the understanding of the electronic structures of high-*Tc* materials. So far, the filled electronic states near the Fermi level of CuO have been measured by photoemission spectroscopy and resonant photoemission spectroscopy,[1,2] while the low-lying unoccupied electronic states of CuO have been studied using Cu-*K*[3,4] and *L*,[5,6] and O-*K*[7] x-ray absorption near-edge structure (XANES) spectroscopy.

In the case of Cu-*K* XANES, there is still uncertainty in the assignment of the observed spectral features to specific electronic transitions, and the role of electron correlation effects in them. To address these issues, detailed angular and polarization dependent Cu-*K* XANES spectra of CuO were reported by Bocharov *et al.*[8] recently for the first time. The data were analyzed theoretically using a real-space multiple-scattering (RS-MS) calculation, which is capable of decomposing the spectra into symmetry-resolved components. The main features of Cu-*K* XANES as well as the weak pre-edge peak were accounted for successfully by the calculation in terms of electric dipole and quadrupole transitions from Cu $1s$ to $4p$-like and $3d$ states, respectively. However, there remain some discrepancies between the calculated spectra and experimental results. Most notably, a prominent spectral feature corresponding to empty $4p_z$-like states was predicted by the theory, but absent in the data. In light of the overall agreement between theory and experiment, this large discrepancy was not expected and attributed to possible many-body processes by the authors.

In this work, high resolution resonant inelastic x-ray scattering (RIXS)[9] study of CuO was carried out. While unoccupied electronic states are routinely studied by x-ray absorption spectroscopy, RIXS offers a complementary view on the electronic structures because RIXS is a second order optical process, and the final states in the absorption process are involved in RIXS as virtual intermediate states. In a previous work, RIXS spectra in the $1s2p$ emission region of several Cu compounds including CuO have been reported.[10] However, because of the low resolution (6 eV) then available, detailed examination of the electronic states was not attempted. With the increase in photon flux and brightness now available at synchrotron radiation facilities, RIXS experiment with much better energy resolution is possible. For example, several high-resolution $1s3p$ RIXS measurements on transition metal compounds including Nd_2CuO_4 (a parent compound of Cu high-*Tc* family)[11,12] have been reported recently.

With much improved energy resolution, 0.2 eV for excitation energy and 1.1 eV for total RIXS measurements, surprisingly complicated spectra were observed. Detailed analysis of these spectra reveals the existence of a new excited state, which is hidden in the Cu-*K* XANES of CuO. Furthermore, the energy of this excited state corresponds well to the $4p_z$-like state predicted by Bocharov *et al.*[8] This result suggests that one-electron interpretation of the Cu-*K* XANES spectra of CuO is adequate and that there is no need to include many-body processes. It also demonstrates the use of RIXS to complement x-ray absorption spectroscopy.

The measurements were carried out at the X21 hybrid wiggler beamline at the National Synchrotron Light Source.[13] The beamline consists of a four-crystal dispersive Si(220) monochromator with miscut angles of $-16°, 0°, 0°, 16°$, a double-focusing mirror, and a horizontally mounted 1 m Rowland circle spectrometer. The energy resolution of the monochromator is 0.2 eV. The monochromatic x rays are then focused onto the sample using a toroidal mirror coated with Pt. The resulting focused beam size is 0.5×0.5 mm^2, and the average incident flux on the sample is $\sim5\times10^{10}$ photons/s. The scattered radiation was analyzed using a spherically bent Si(444) crystal, and detected by a Si PIN diode. To acquire the inelastic spectra, the rotation of the analyzer and the translation of the detector were synchronized to follow the Rowland circle. Also, in these measurements, the active area of the analyzer was limited to 45 mm in diameter, which resulted in the overall energy

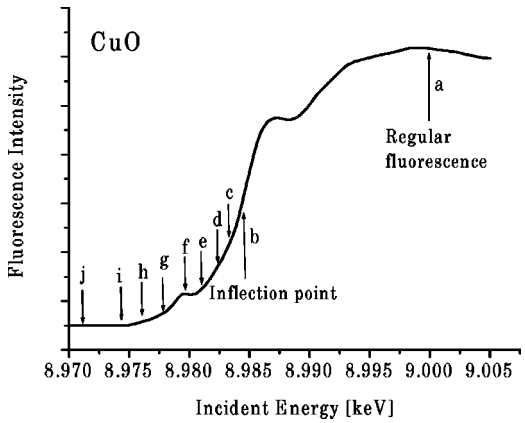

FIG. 1. Fluorescence XANES spectrum of CuO. The arrows and labels (a)–(j) indicate the excitation energies at which high-resolution RIXS spectra were measured.

resolution (ΔW_{res}) of 1.1 eV as determined by the FWHM of the elastic line. In addition, CuO XANES spectrum was obtained by monitoring total fluorescent yield as a function of incident x-ray energy. Finally, all data reported here were taken on a CuO powder sample at room temperature, and at a constant scattering angle of 40°.

Figure 1 shows the fluorescent yield XANES spectrum of CuO. A weak pre-edge peak at ~8980 eV is observed. This peak is a well-known spectral feature due to Cu $1s \rightarrow 3d$ transition,[3,4] which is characteristic of divalent copper compounds, and is expected to be absent in monovalent copper compounds because their $3d$ orbitals are fully occupied. At slightly higher energy, a steep rise in absorption coefficient due to the Cu-*K* absorption edge is observed. The energy of the inflection point, the conventional definition of absorption edge, is about 8984.3 eV. The arrows and labels in Fig. 1 indicate the excitation energies ($\hbar\omega_1$) at which high-resolution RIXS spectra were measured.

Figure 2 shows the RIXS spectra of CuO as a function of the scattered photon energy ($\hbar\omega_2$) for various excitation energies ($\hbar\omega_1$). Excitation with x-ray energies well above the *K*-absorption edge energy yields two bands at 8047.8 eV and 8027.8 eV, which are the well-known Cu-$K\alpha_1$ and $K\alpha_2$ fluorescence lines. As the excitation energy lowered to 8984.3 eV, the inflection point of the absorption spectrum, two main features corresponding to the $K\alpha$ doublet (denoted A and A′) are observed. In comparison with the $K\alpha$ doublet, the energies of A and A′ are shifted down by about 1 eV, and their widths are broadened slightly. In addition, a new feature, labeled S, appears between A and A′. By lowering the excitation energy to just 1 eV below the inflection point energy, a new pair of bands accompanying A and A′, labeled B and B′, is clearly observed. There is also the appearance of another very weak pair of bands at the high-energy side of B and B′, labeled C and C′.

As the excitation energy further decreases from the absorption edge energy, systematic evolution of these spectral features are observed as shown in curves d–j. For A and A′, the peak energies continue to shift to lower energy in accordance with the decrease in excitation energy, preserving the energy loss ($E_{\mathrm{loss}}=\hbar\omega_1-\hbar\omega_2$) of 936 eV (A) and 956 eV

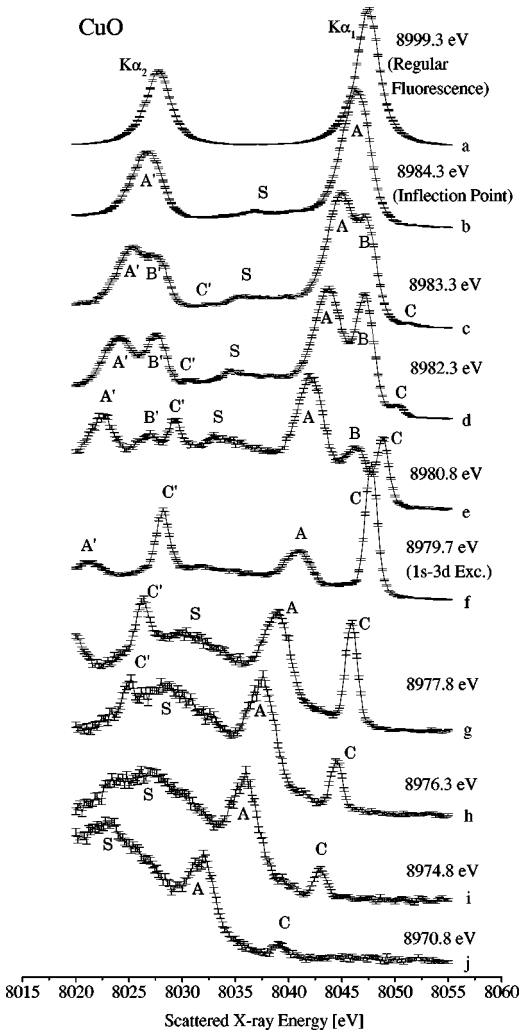

FIG. 2. $1s2p$ RIXS spectra of CuO. Each spectrum is normalized using its maximum value.

(A′), respectively. At the same time, the scattering intensities also decrease monotonically. In contrast to the simple trend observed for A (A′), B and B′ are only observable within a very small range of excitation energy, 8980.8–8983.3 eV, and their intensities go through a maximum at the excitation energy of 8982.3 eV. Furthermore, it should be noted that E_{loss} of the bands B and B′ varies with the excitation energy as is evidenced from the variation of energy splitting between B (B′) and A (A′).

Similar behavior is observed for the bands C and C′. However, E_{loss} for C (932 eV) and C′ (952 eV) remain constant and independent of the excitation energy. It is interesting to note that at the excitation energy of 8979.7 eV, the width of the C (C′) is the narrowest, and considerably narrower than that of the regular $K\alpha$ lines. The FWHM of C in the raw data (ΔW_{obs}) is 1.21 ± 0.15 eV while that of the regular $K\alpha_1$ line is 2.46 ± 0.15 eV. After correction for the instrumental resolution using $\sqrt{\Delta W_{\mathrm{obs}}^2-\Delta W_{\mathrm{res}}^2}$, the FWHM of C and $K\alpha_1$ are about 0.5 eV and 2.2 eV, respectively. Finally, the weak and broad band denoted S in the spectrum persists with decreasing excitation energy similar to A and A′.

The differential cross section of the RIXS process, where a transition from the initial state $|i\rangle$ to the final state $|f\rangle$ takes place through virtual intermediate states $|n\rangle$ while the photon energy changes from $\hbar\omega_1$ to $\hbar\omega_2$, can be described by the well-known Kramers–Heisenberg equation, which can be further reduced to[14]

$$\frac{d\sigma(\omega_1)}{d\omega_2} \propto \int \left[\frac{\omega_2}{\omega_1}\right] \frac{(\Omega_{1s}-\Omega_{2p}) g_{2p,1s}(\Omega_{1s}+\omega)(dg_{1s}/d\omega)}{(\Omega_{1s}+\omega-\omega_1)^2+\Gamma_{1s}^2/4\hbar^2} \times \delta(\omega_1-\Omega_{2p}-\omega-\omega_2)d\omega, \quad (1)$$

where

$$\delta(\omega_1-\Omega_{2p}-\omega-\omega_2) = \frac{\Gamma_{2p}/2\pi\hbar}{(\omega_1-\Omega_{2p}-\omega-\omega_2)^2+\Gamma_{2p}^2/4\hbar^2}. \quad (2)$$

Here $\hbar\omega$ is the kinetic (positive) or binding (negative) energies of the excited electron in the virtual intermediate state $|n\rangle$, and Γ_{1s} and Γ_{2p} are the lifetime widths of the $1s$ and $2p$ levels, the binding energies of which are represented by $\hbar\Omega_{1s}$ and $\hbar\Omega_{2p}$. The oscillator strength of the transition between the $1s^{-1}$ and $2p^{-1}$ hole states is given by $g_{2p,1s}$, and $dg_{1s}/d\omega$ is the density of unoccupied states which is in general a superposition of discrete and continuous features. In short, the resonant inelastic scattering spectrum reflects the density of unoccupied states modified by the energy denominator and Eq. (2). A schematic energy diagram showing all the relevant energy levels is shown in Fig. 3(a).

In the previous study[10] the density of unoccupied states, $dg_{1s}/d\omega$, was assumed to be a step function and RIXS spectra were calculated by the use of Eqs. (1) and (2). This simple approximation was able to reproduce the gross features of the RIXS spectra, including the gradual excitation energy dependence of the scattering intensity, the energy shifts as a function of excitation energy, and the changes in band shape as the deviation from the rigorous resonance condition increases. In fact, the excitation energy dependence of bands A and A′ observed in the present work can still be completely interpreted within this approximation. However, in order to understand the complex behavior of the bands B (B′) and C (C′), detailed spectral features in CuO XANES has to be taken into consideration.

First, the scattering intensities of bands C and C′ are the strongest for excitation energy $\hbar\omega_1 = 8979.7$ eV, which corresponds exactly to the $1s \rightarrow 3d$ transition energy. Since $\hbar\omega_1 = \hbar(\Omega_{1s}+\omega_{3d})$, the denominator in Eq. (1) satisfies the resonant condition for $\omega = \omega_{3d}$, which accounts for the intensity maximum at this excitation energy. At the same time, the delta function in Eq. (1) predicts the maximum scattered intensity at $\hbar\omega_2 = \hbar(\Omega_{1s}-\Omega_{2p})$. This interpretation also predicts that with detuning $\hbar\omega_1$ by $\hbar\varepsilon$ to either higher or lower energy, the intensity decreases and $\hbar\omega_2 = \hbar(\Omega_{1s} - \Omega_{2p} - \varepsilon)$ decreases or increases depending upon the sign of ε, which agree well with observed excitation dependence of energies and intensities of the C and C′ bands. The analysis above clearly suggests that the scattering strength of bands C and C′ are originated from the virtual $(1s)^{-1}(3d)^{10}$ intermediate state.

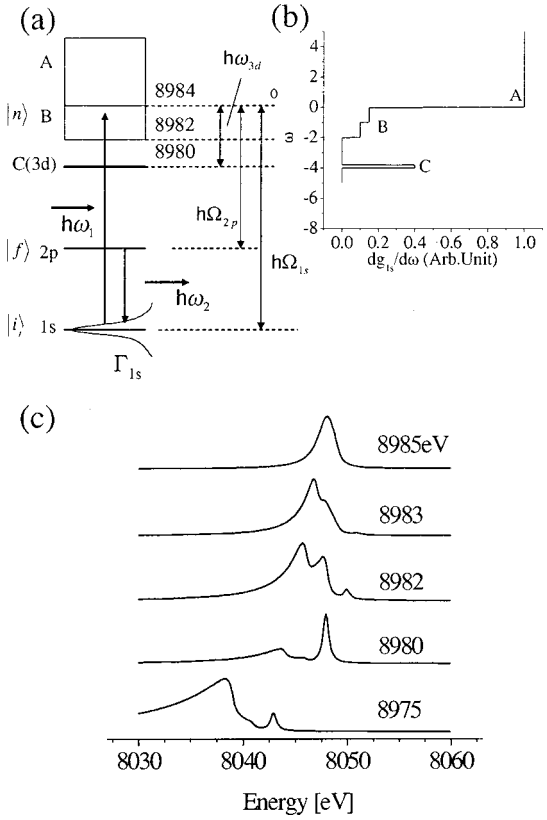

FIG. 3. (a) An energy diagrams of CuO and (b) a model density of unoccupied states for CuO. Unoccupied states consist of a narrow band (C) corresponding to the vacant $3d$ state, a band with a finite width (B), and a step-function like continuum (A). (c) Calculated RIXS spectra for several excitation energies using model density of states (b).

It is also interesting to note that the bandwidth of the peak C and C′ at $\hbar\omega_1 = 8979.7$ eV is much narrower than the lifetime width of the Cu $1s$ core hole. Close examination of Eqs. (1) and (2) shows that under exact resonant condition, $\hbar\omega_1 = \hbar(\Omega_{1s}+\omega_{3d})$, the band width is determined only by Γ_{2p} and does not depend on Γ_{1s}. Indeed, the FWHM value of C after corrected for the instrumental resolution, 0.5 eV, shows a very good agreement with the semiempirical $\Gamma_{2p3/2}$ value, 0.56 eV.[15]

The interpretation of the bands B and B′ is not as straightforward since there is no clear XANES feature in the narrow energy range that B and B′ are observed. Specifically, the bands B and B′ were observed only for $\hbar\omega_1$ between 8980.8 eV and 8983.3 eV. Below $\hbar\omega_1 = 8979.8$ eV no peak corresponding to the band B was observed. In addition, unlike the bands A and C, their energy losses depend on the excitation x-ray energy. This behavior of the bands B and B′ can be understood only if the existence of a bound unoccupied electronic state with finite width is assumed between the $3d$ peak (~8980 eV) and the inflection point (~8984 eV).

In order to confirm the hypothesis above, calculations assuming different model density of states were attempted.

One of the models is shown in Fig. 3(b), where in addition to a step function with edge energy of 8984 eV, a delta-function centered at 8984 eV and two step functions with edge energies of 8982 eV and 8983 eV are assumed. The delta-function (a 0.2 eV wide square was employed for numerical calculations) is used to represent the unoccupied $3d$ states, and the latter two step functions are included to approximate the unknown near edge structures. We then calculated the RIXS spectra using this model density of states together with Eqs. (1) and (2). Figure 3(c) shows the calculated RIXS spectra for several excitation energies. A comparison of Fig. 3(c) with Fig. 2 demonstrates that the observed excitation energy dependences of bands A, B, and C agree well the calculation, indicating that the assumed density of states is a fairly good model for the unoccupied electronic states of CuO.

In fact, the presence of a weak bound state between 8980.8 eV and 8983.3 eV has been suggested, but has not been observed up to now. For example, in a recent combined polarized XANES and real-space multiple-scattering calculation study of CuO, Bocharav *et al.*[8] concluded that although the gross features of polarized XANES spectrum can be reproduced by the calculation, some discrepancies between experiment and theory still remain, the most significant one being the absence of the Cu $1s$ to $4p_z'$ dipole transition near 8983 eV in the experimental absorption spectra. In their convention, the z' axis is perpendicular to the CuO_4 parallelogram plane. Our observation here clearly supports the calculation that there is an unoccupied state at ~8983 eV in spite of the absence of distinct peak or shoulder in the x-ray absorption spectrum.

Unfortunately, it is not possible with present experimental results from a powder sample to determine whether the transition is to the p_z' orbital or not. However, L_3 absorption studies[5,6] on CuO show that there is no marked structure at high energy side of the strong peak due to the $2p \rightarrow 3d$ transition, which suggests that the character of the state giving the band B (B′) is neither *s* nor *d*, but *p* dominant. Polarization dependent RIXS measurements on single crystal CuO samples will be performed to unambiguously determine the symmetry of these states.

In summary, we report a high resolution RIXS study on CuO. With improved energy resolution and model calculations, a weak unoccupied electronic state of CuO is uncovered. Even for features observable in normal x-ray absorption spectrum, for example the Cu $1s$ to $3d$ pre-edge peak, RIXS spectra also have superior signal-to-background ratio. These results demonstrate the potential use of RIXS, especially polarization dependent RIXS measurements on single crystal samples, to provide valuable new information on the electronic structures of transition metal compounds, as well as stringent tests for electronic structure calculations for these systems.

National Synchrotron Light Source is supported by U.S. Department of Energy under Contract No. DE-AC02-98CH10886.

*Author to whom correspondence should be addressed. Tel: +81-22-217-5385; Fax: +81-22-217-5405; Electronic mail: hayashi@tagen.tohoku.ac.jp

[1] J. Ghijsen, L. H. Tjeng, H. Eskes, G. A. Sawatzky, and R. L. Johnson, Phys. Rev. B **42**, 2268 (1990).
[2] L. H. Tjeng, C. T. Chen, J. Ghijsen, P. Rudolf, and F. Sette, Phys. Rev. Lett. **67**, 501 (1991).
[3] F. W. Lytle, R. B. Greegor, and A. J. Panson, Phys. Rev. B **37**, 1550 (1988).
[4] N. Kosugi, H. Kondoh, H. Tajima, and H. Kuroda, Chem. Phys. **135**, 149 (1989).
[5] M. Grioni, J. B. Goedkoop, R. Schoorl, F. M. F. deGroot, J. C. Fuggle, F. Schäfers, E. E. Koch, G. Rossi, J.-M. Esteva, and R. C. Karnatak, Phys. Rev. B **39**, 1541 (1989).
[6] L. H. Tjeng, C. T. Chen, and S.-W. Cheong, Phys. Rev. B **45**, 8205 (1992).
[7] M. Grioni, M. T. Czyzyk, F. M. F. deGroot, J. C. Fuggle, and B. E. Watts, Phys. Rev. B **39**, 4886 (1989).
[8] S. Bocharov, Th. Kirchner, G. Dräger, O. Šipr, and A. Šimůnek, Phys. Rev. B **63**, 045104 (2001).
[9] A. Kotani and S. Shin, Rev. Mod. Phys. **73**, 203 (2001).
[10] Y. Udagawa, H. Hayashi, K. Tohji, and T. Mizushima, J. Phys. Soc. Jpn. **63**, 1713 (1994).
[11] J. P. Hill, C. C. Kao, W. A. L. Caliebe, M. Matsubara, A. Kotani, J. L. Peng, and R. L. Greene, Phys. Rev. Lett. **80**, 4967 (1998).
[12] K. Hämäläinen, J. P. Hill, S. Huotari, C. C. Kao, L. Berman, A. Kotani, T. Ide, J. L. Peng, and R. L. Greene, Phys. Rev. B **61**, 1836 (2000).
[13] H. Hayashi, Y. Udagawa, J. M. Gillet, W. A. Caliebe, and C.-C. Kao, *Chemical Application of Synchrotron Radiation* (World Scientific, Singapore, 2002), Chap. 18.
[14] J. Tulkki and T. Åberg, J. Phys. B **15**, L435 (1982).
[15] M. O. Krause and J. H. Oliver, J. Phys. Chem. Ref. Data **8**, 329 (1979).